Critical parameters to obtain Yb3+ doped Lu2O3 and ZnO transparent ceramics

Mythili Prakasam, Oudomsack Viraphong, Dominique Michau, Alain Largeteau

Critical parameters to obtain Yb^{3+} doped Lu_2O_3 and ZnO transparent ceramics

Prakasam M.[a,b], Viraphong O.[a,b], Michau D.[a,b], Largeteau A.[a,b]
[a] Univ. Bordeaux, ICMCB, UPR 9048, F-33600 Pessac, France
[b] CNRS, ICMCB, UPR 9048, F-33600 Pessac, France

Abstract :

Transparent ceramics of zinc oxide (ZnO) and 10% Yb^{3+} doped Lu_2O_3 (YLO) were fabricated by spark plasma sintering. The major sintering parameters to obtain transparent ceramics and their interdependency on each other are explained for cubic and non-cubic crystal structured transparent ceramics. Highly densified YLO and ZnO ceramics were obtained at 1250 °C and 850 °C, respectively. Postannealing of sintered YLO and ZnO ceramics at 1200 °C and 700 °C respectively removes discoloration and improves transparency. The 2 mm thick YLO ceramics prepared at 1700 °C with dwell time of 5 min and heating rate at 50 °C/min shows the maximum transmittance of 55% at a wavelength of 2 µm and the 2 mm thick ZnO transparent ceramics prepared at 1100 °C with dwell time of 20 min and heating rate of 10 °C/min shows maximum transmittance in the visible region with nearly 60% transmittance.

1. Introduction

Transparent ceramics are widely studied owing to their versatility in various optoelectronic applications. Few cubic crystal system materials such as magnesium-aluminate spinel and sesquioxides have been realized in the form of transparent ceramics. Non-cubic crystal structures are mostly processed in the form of polycrystalline materials, as anisotropic grains could cause considerable light scattering around grain boundaries resulting in light absorption, inhibiting transparency in the fabricated ceramics. Non-cubic crystal structured materials need an equilibrium with various sintering parameters such as sintering temperature, dwell time, pressure and grain size to fabricate as transparent ceramics. To obtain transparent ceramics, consolidation of micro/nanograined powders is done at high temperatures with simultaneous application of high pressure (either by hot pressing (HP) or as hot isostatic pressing (HIP) [1], [2] and [3]). Maximum transparencies up to 85% have been achieved with the aforesaid techniques either by addition of additives or with comparatively slower heating rates than spark plasma sintering.

Spark plasma sintering (SPS), is relatively a decade old technique which implements conjoint application of axial pressure at high temperature, initiated by DC pulses. The joule energy from the DC pulses enhances surface activation of grains by raising the temperature on the surface of each grain, which leads to highly densified samples at lower sintering temperatures and dwell time. Though SPS is currently being used for various groups of materials, its application in the field of transparent ceramics is limited [4]. Highly transparent ceramics with controlled microstructures by SPS have been prepared by a two-step pressure profile, i.e., a low pre-loading pressure at low temperatures and a high pressure at high temperatures [5]. The heating rate is another important sintering parameter for densification in the second and third stages. Although a fast heating rate >30 °C/min is widely used in SPS, a low heating rate was applied to fabricate highly transparent Al_2O_3[6] and $MgAl_2O_4$[5]. SPS densified polycrystalline oxides generally fail to yield transmittance expected by theoretical inline transmittance, especially in the ultraviolet and low visible wavelengths. This optical behavior may be principally due to the presence of pores that are often observed at the

grain junctions of ceramics subjected to SPS. In addition, another drawback is the reduction condition in SPS due to the presence of graphite at high temperature in vacuum. It has been reported that the combination of two-step profile and low heating rate can be more advantageous to obtain fine microstructure bodies with improved transparencies [7].

In the present work, we study about the various parameters yielding transparent ceramics of cubic crystal structured Yb^{3+} doped Lu_2O_3 (YLO) and non-cubic crystal structured (hexagonal) zinc oxide (ZnO) by SPS. Lu_2O_3 is a sesquioxide with cubic crystal structure which has applications in scintillation detectors and laser gain media. Lu_2O_3:Yb^{3+} crystals exhibit a potential to replace Yb^{3+}: YAG for 976 nm diode pumped high-power laser applications. But these types of crystals are difficult to be grown due to the high temperature growth issues, which limit size and quality. Further ZnO is a material with unique combination of semiconductor material with a significant fraction of ionic bonding. ZnO powder and thin films are commonly employed in scintillators, where large volume and high transparency in the spectral range of emission is required. It has to be noted that to obtain ZnO single crystal is a long and expensive technological process. Thus optical ceramics, in the form of polycrystalline material could be an attractive choice to single crystals to be implemented for scintillators. Recently Taira et al. [8] and [9] have reported about a new means for anisotropic ceramics. Though transparent ceramics of ZnO [10], [11], [12], [13], [14] and [15] are fabricated by other techniques, SPS technique was preferred by us due to its rapid heating rate and time-effectiveness. This article focuses on the various parameters catered to yield good quality transparent ceramic of YLO and ZnO, with shorter processing time and lower sintering temperature than obtained with other conventional ceramic processing techniques and crystal growth methods.

2. Experimental procedure

Due to commercial non availability of 10% Yb^{3+} doped Lu_2O_3 (YLO) powder, YLO nanopowders were synthesized by the co-precipitation method. The detailed procedure is reported elsewhere [16]. Commercially available ZnO was procured from Alfa Aesar, which was sieved to obtain grain size≈50 µm. For each experiment 2 g of YLO and ZnO powder was filled into graphite die having an inner diameter of 8 mm. The graphite die was covered with a thermal insulator carbon fiber to avoid contamination from the graphite die to the starting powder. An optical pyrometer was used to measure temperature on the graphite die surface. The graphite mold was placed in SPS operating chamber (DR. SINTER LAB Spark Plasma Sintering system, Model SPS-511S/SPS-515S) under Vacuum of 10^{-6} Torr. The pulse sequence for SPS applied voltage for all the samples was 12:2 (i.e. 12 ON/2 OFF). The shrinkage of the densifying powder was continuously monitored by the displacement of the punch rod. The temperature was first increased to 600 °C within 3 min and then increased to a range of temperatures from 1400 °C to 1800 °C for YLO and 900 °C to 1100 °C for ZnO with different heating rates (R_H) ranging from 5 °C/min to 200 °C/min and dwell time. Uniaxial pressures ranging from 40 MPa to 100 MPa were applied at room temperature (T_R) and sintering temperatures (T_S) and their significances have been analyzed. The cooling rate (R_C) and R_H were maintained equal in all the experiments. The higher value of R_H and higher value of R_C lead to opacity and cracking in ceramics. The SPS densified ceramics of YLO and ZnO obtained were black in color, due to the reducing nature of SPS experimental process and porosity. The thermal insulator layer on the ceramics was removed and the ceramics were annealed at 900 °C for YLO ceramics and 700 °C for ZnO ceramics during 1 h in air to compensate the lost oxygen in SPS chamber. Then the ceramics were mirror polished on both sides using diamond slurry. The thickness of the ceramics after polishing was approximately 2 mm. The obtained transparent ceramics of ZnO and YLO are shown in Fig. 1. The density and porosity were measured by in distilled water by Archimede's method. The microstructure was observed by a scanning electron microscope (Jeol 840 SEM). The optical transmittance spectrum was measured by using a double beam spectrophotometer (Varian Cary 5000) at a range of between 200 and 3000 nm.

3. Results and discussion

In order to obtain transparent ceramics, the various vital parameters such as grain size, grain-boundary phase and pores has to be dealt with. It has been reported that higher transmittance in ceramics can be obtained, if it is pore free and is independent of the grain size [17]. We observed that the YLO and ZnO densification depends on the sintering temperature employed. The transparency of YLO and ZnO ceramics are influenced by pressure as well, which was observed (1) by applying constant maximum pressure (P_s) in the entire process. (2) By applying P_s during the dwell time (t_s). Significant increase in densification was observed, when P_o=P_s. High pressure also accelerates densification by plastic deformation leading to second sintering stage [18] and [19]. We observed that when pressure was increased to 100 MPa, the relative density gradually reaches above 95% for YLO and 97% for ZnO (Fig. 2), with increasing t and T_S. Small increase in density after attaining saturated densification temperature might be mainly due to grain boundary diffusion associated with grain growth.

The next aspect taken into consideration was grain growth dependence on sintering temperature and applied pressure. In YLO and ZnO ceramics, we observed that the maximum densification was observed at 1250 °C and 900 °C, above these temperatures, the densification remains stable. It is well known that when a dense body is held at high temperature for long time, it leads to grain growth. Yet the report [18] has shown that laser oscillation was demonstrated in the relatively large grain size of ~50 μm, still large grained materials cannot render efficiency demanding high thermal shock resistance, such as high energy laser systems that can generate massive heat loads. We employed two-stage sintering [20] and [21] based on thermodynamical point of view to minimize the grain growth. Accordingly, there is an active temperature range which enlivens grain boundary diffusion, but limiting grain boundary migration hence leading to further increase in densification without any significant grain growth. We could control the average grain sizes of YLO and ZnO ceramics differing over a range of 10 nm–5 μm.

Another indispensable aspect studied to obtain transparent ceramics was the influence of heating rate on pore formation and grain size homogeneity. It was observed that in YLO and ZnO ceramics, even though when R_H is >50 °C/min, sintering pressure effects in yielding higher densification at the end stage of sintering. Pores were observed at the triple junctions of grain boundaries. The number of pores increased with R_H>50 °C/min. The average size of the grain increases rapidly with increasing R_H, leading to inhomogeneous grain size distribution inhibiting transparency of the ceramic. Large stress formed among the grains leads to inhomogeneous and large average grain size at higher R_H[22]. In YLO ceramics, we observed that the formation of pore and increase of grain size is predominant at R_H>50 °C/min and as well as at R_H<50 °C/min, irrespective of t_s. In ZnO ceramics, R_H>10 °C/min leads to a significant increase in grain size. The optimal R_H to yield transparent YLO ceramics was determined to be R_H=50 °C/min and R_H=10 °C/min for ZnO ceramics. There are similar reports [23], [24], [25], [26] and [27] on Al_2O_3 ceramics prepared by SPS ascertaining a possibility of grain boundary diffusion and creep densification, yielding smaller grain growth at higher R_H than at lower R_H. Aforesaid is valid for YLO at R_H>50 °C/min. Whereas in the regime, when R_H<50 °C/min for YLO (as opposed to ZnO), lower R_H leads to greater possibility to have larger grain growth, a similar trend has been reported for Y_2O_3 ceramics prepared by SPS. We further observed that the crack is not observed in the sintered samples with R_H=R_C. In the case of lower R_H and higher R_C or vice versa, there is crack on the surface of the sintered body, which is applicable for both YLO and ZnO ceramics.

A slight discoloration is observed in most of transparent ceramics fabricated by SPS such as ZrO_2, Al_2O_3 and $MgAl_2O_4$, which arises due to the reducing atmosphere leading to oxygen vacancies formed during SPS [24] and at higher heating rate. In the present study, all the sintered YLO ceramics were annealed at 1200 °C for 12 h and ZnO ceramics were annealed at 700 °C for 5 h. During the annealing process, oxygen vacancies are compensated, resulting in its discoloration and also enhances transparency (particularly in the visible range). When the annealing temperature is increased above 1200 °C and 700 °C for YLO and ZnO ceramics respectively, leads to opacification of the ceramics due to the increase in porosity and abnormal grain growth.

All the ceramics fabricated were slightly gray in color. The color gradually lightens with increase in temperature. With slight changes in density at higher temperatures leads to increased transmittance at higher temperature, being insensitive to porosity. Fig. 3 shows the SEM micrographs of transparent YLO and ZnO ceramics sintered at P_S=100 MPa, R_H=50 °C/min, and T_S=1700 °C (t_s=5 min); for ZnO ceramics P_S=100 MPa, R_H=10 °C/min, and T_S=1100 °C (t_s=20 min). From the microstructures of YLO and ZnO ceramics, we observed that the average grain size decreases with increasing P_S. It has to be emphasized that irrespective of the grain size, if the residual pores are very minimal, then ceramic could be translucent/mildly transparent. In Fig. 4, variation of microstructure with pressure and dwell time for ZnO optical ceramics is shown. Fig. 4(a) is the microstructure of ZnO where the maximum pressure was applied during the dwell time and held until the end of dwell time, leads to minimum pores around the grain boundaries. Fig. 4(b) shows the microstructure of ZnO, when maximum pressure is applied at dwell time and held until the end of cooling cycle, leads to formation of pores at the triple junctions and also between intergranular regions (with the increase of dwell time, the pore size increases). Fig. 4(c) shows the optimized conditions to obtain transparent ceramics of ZnO, where the pressure was applied at dwell time and released at the end of dwell time. There are no porosities observed between the grains leading to an increase in transparency. Fig. 4(d) and (f) shows the microstructures of ZnO with the application of maximum pressure with the start of heat cycle and held during complete experiment cycle and only during heating cycle, respectively. However the application of pressure during the start of the experiment cycle and released during the cooling cycle, the pore formation is restricted mostly in inter granular region as can be seen in Fig. 4(e). In the present investigation, we obtained nearly higher transmittance [16] as that was reported for HIP yielded YLO ceramics and increased transmittance for ZnO ceramics (Fig. 5) existing in the literature, at lesser temperature and short processing time than in conventional sintering processes. Fig. 5 implies that the maximum transmittance is obtained in the visible region with nearly 60% transmittance for ZnO transparent ceramics fabricated by SPS.

In general, residual pores which are in the same size range as the incident wavelength act as efficient scattering source at a corresponding wavelength. We have noted that the apparent porosity of YLO ceramics decreases with increasing temperatures and increasing holding time, while the applied pressure has little effect on the porosity because of the high hardness.

4. Conclusion

Transparent YLO and ZnO ceramics with high density has been fabricated by SPS. The sintering parameters and their various effects on different factors of ceramics have been investigated. The complete densification was obtained at 1250 °C and 850 °C for YLO and ZnO ceramics respectively. Transparent YLO ceramics were obtained at 1700 °C (t_s=5 min) at 100 MPa, with R_H=50 °C/min and ZnO transparent ceramics were obtained at 1100 °C (t_s=20 min) at 100 MPa, with R_H=10 °C/min. A homogeneous microstructure was observed in the fabricated ceramics. The YLO ceramics had nearly 5–10% improvement in transmittance upon post-annealing at 1200 °C for 12 h, whereas ZnO ceramics had 5% improvement upon postannealing at 700 °C for 5 h. The discoloration disappears at annealing temperature of 1200 °C, compensating oxygen vacancies, being the optimal temperature for post-annealing YLO ceramics. SPS technique yielded YLO and ZnO transparent ceramics at comparatively lesser temperature and processing time. Further investigations are in progress to study the optical properties of the fabricated ceramics by SPS.

References

1. P. Hing. Fabrication of translucent magnesium aluminate spinel and its compatibility in sodium vapor. Journal of Materials Science, 11 (1976), pp. 1919–1926.
2. M. Shimada, T. Endo, T. Saito, T. Sato. Fabrication of transparent spinel polycrystalline materials. Materials Letters, 4 (1996), pp. 413–415.

3. J.S. Sanghera, W. Kim, C. Baker, G. Villalobos, J. Frantz, B. Shaw, A. Lutz, B. Sadowski, R. Miklos, M. Hunt, F. Kung, I. Aggarwal. Laser oscillation in hot pressed 10% Yb^{3+}:Lu_2O_3 ceramic. Optical Materials, 33 (2011), pp. 670–674.
4. Z.A. Munir, U. Anselmi-Tamburini, M. Ohyanagi. The effect of electric field and pressure on the synthesis and consolidation of materials: a review of the spark plasma sintering method. Journal of Materials Science, 41 (2006), pp. 763–777.
5. C. Wang, Z. Zhao. Transparent $MgAl_2O_4$ ceramic produced by spark plasma sintering. Scripta Materialia, 61 (2009), pp. 193–196.
6. B.-N. Kim, K. Hiraga, K. Morita, H. Yoshida. Spark plasma sintering of transparent alumina. Scripta Materialia, 57 (2007), pp. 607–610.
7. K. Morita, B.-N. Kim, H. Yoshida, K. Hiraga. Spark-plasma-sintering condition optimization for producing transparent $MgAl_2O_4$ spinel polycrystals. Journal of the American Ceramic Society, 92 (2009), pp. 1208–1216.
8. Takunori Taira. Optical Materials Express, 1 (15) (2011), pp. 1040–1050.
9. Jun Akiyama, Yoichi Sato, Takunori Taira. Optics Letters, 35 (2010), pp. 3598–3600.
10. D.R. Clarke. Varistor ceramics. Journal of the American Ceramic Society, 82 (1999), pp. 485–502.
11. T. Senda, R.C. Bradt. Grain growth in sintered ZnO and ZnO–Bi_2O_3 ceramics. Journal of the American Ceramic Society, 73 (1990), pp. 106–114.
12. D. Dey, R.C. Bradt. Grain growth of ZnO during Bi_2O_3 liquid-phase sintering. Journal of the American Ceramic Society, 75 (1992), pp. 2529–2534.
13. E. Olsson, G.L. Dunlop. The effect of Bi_2O_3 content on the microstructure and electrical properties of ZnO varistor materials. Journal of Applied Physics, 66 (1989), pp. 4317–4324.
14. J. Langer, M.J. Hoffmann, O. Guillon. Electric field-assisted sintering and hot pressing of semiconductive zinc oxide: a comparative study. Journal of the American Ceramic Society, 94 (2011), pp. 2344–2353.
15. T. Misawa, N. Shikatani, Y. Kawakami, T. Enjoji, Y. Ohtsu, H. Fujita. Observation of internal pulsed current flow through the ZnO specimen in the spark plasma sintering method. Journal of Materials Science, 44 (2009), pp. 1641–1651.
16. Mythili Prakasam, Oudamsack Viraphong, Dominique Michau, Philippe Veber, Matias Velázquez, Kiyoshi Shimamura, Alain Largeteau. Yb^{3+} doped Lu_2O_3 transparent ceramics by spark plasma sintering. Ceramics International, 39 (2013), pp. 1307–1313.
17. A. Ikesue, T. Kinoshita, K. Kamata, K. Yoshida. Fabrication and optical properties of high-performance polycrystalline Nd:YAG ceramics for solid-state laser. Journal of the American Ceramic Society, 78 (1995), pp. 1033–1040.
18. R. Chaim, M. Levin, A. Shlayer, C. Estournes. Sintering and densification of nanocrystalline ceramic oxide powders: a review. Advances in Applied Ceramics, 107 (2008), pp. 159–169.
19. S. Hosokawa, H. Yagi, T. Yanagatani, Translucent lutetium oxide sinter, and method for manufacturing the same, US Patent #7,597, 2009, pp. 866.
20. I.W. Chen, X.H. Wang. Sintering dense nanocrystalline ceramics without final-stage grain growth. Nature, 404 (2000), pp. 168–171.
21. X.H. Wang, P.L. Chen, I.W. Chen. Two-step sintering of ceramics with constant grain-size, I. Y_2O_3. Journal of the American Ceramics Society, 89 (2006), pp. 431–437.
22. C.-W. Li, S.-C. Lui, J. Goldacker. Relation between strength, microstructure, and grain-bridging characteristics in in situ reinforced silicon nitride. Journal of the American Ceramics Society, 78 (1995), pp. 449–459.
23. Z.J. Shen, M. Johnsson, Z. Zhao, M. Nygren. Spark plasma sintering of alumina. Journal of the American Ceramics Society, 85 (2002), pp. 1921–1927.
24. D.T. Jiang, D.M. Hulbert, U. Anselmi-Tamburini, T. Ng, D. Land, A.K. Mukherjee. Optically transparent polycrystalline Al_2O_3 produced by spark plasma sintering. Journal of the American Ceramics Society, 91 (2008), pp. 151–154.
25. E.A. Olevsky, S. Kandukuri, L. Froyen. Consolidation enhancement in spark-plasma sintering: impact of high heating rates. Journal of Applied Physics, 102 (2007), pp. 114913–114925.
26. N. Murayama, W. Shin. Effect of rapid heating on densification and grain growth in hot pressed alumina. Journal of the Ceramics Society Japan, 108 (2000), pp. 799–807.
27. B.-N. Kim, K. Hiraga, K. Morita, H. Yoshida.Effects of heating rate on microstructure and transparency of spark-plasma-sintered alumina. Journal of the European Ceramics Society, 29 (2009), pp. 323–327.

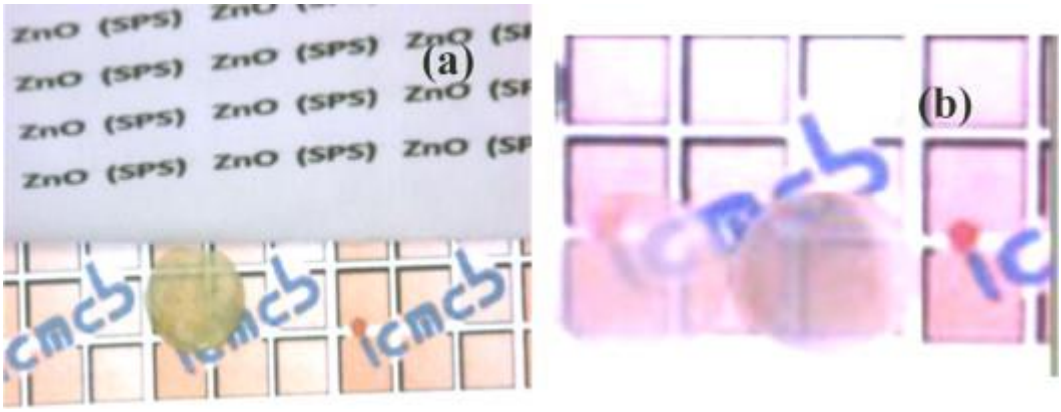

Fig. 1. Transparent ceramics of (a) ZnO and (b) YLO fabricated by spark plasma sintering.

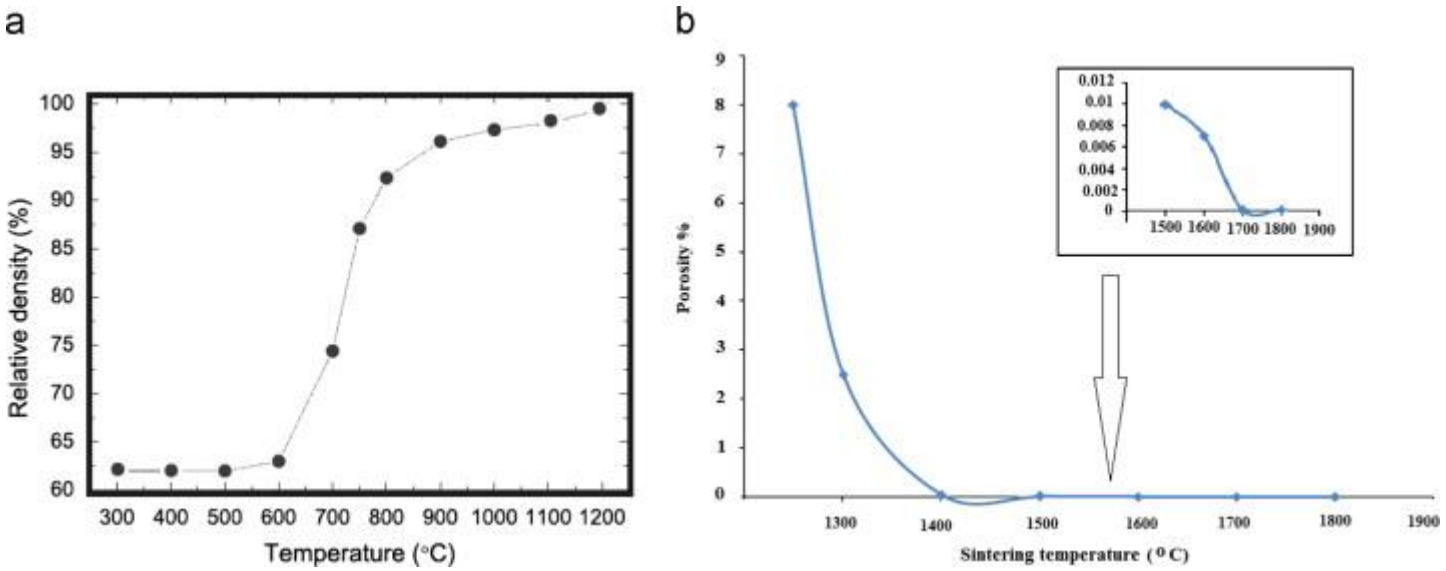

Fig. 2. (a) Dependence of relative density of ZnO ceramics with temperature. (b) Dependence of porosity with sintering temperature for YLO ceramics.

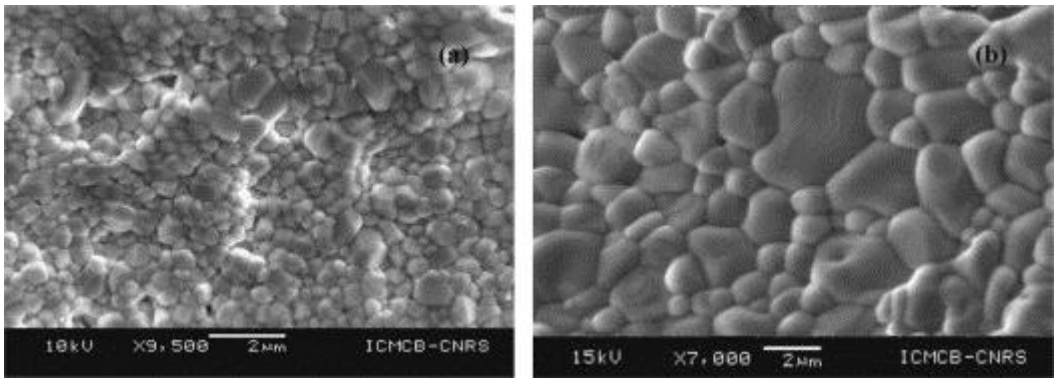

Fig. 3. Micrographs of (a) YLO ceramics sintered at 1700 °C for 5 min with heating rate of 50 °C/min and (b) ZnO ceramics sintered at 1100 °C for 20 min with heating rate of 10 °C/min.

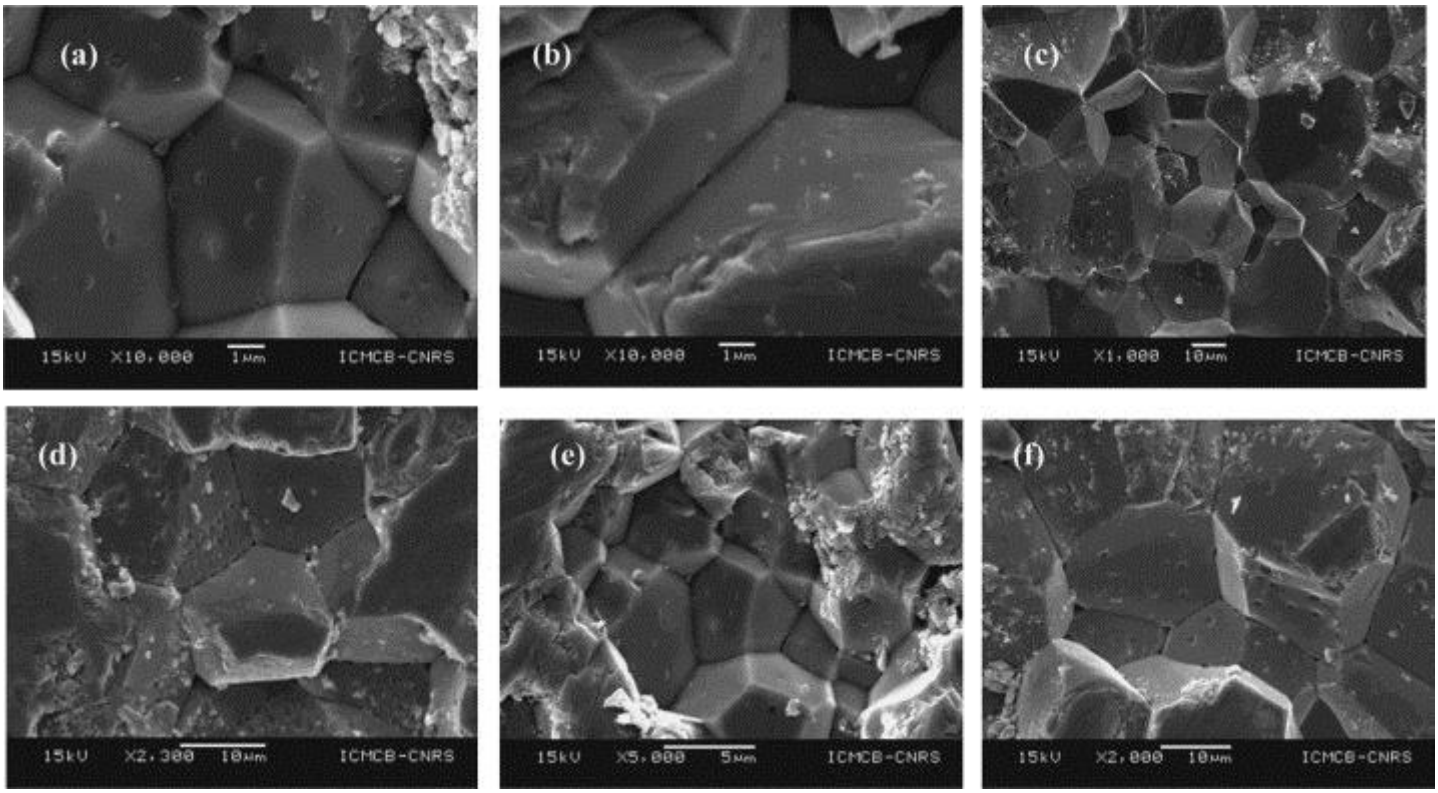

Fig. 4. Evolution of micrographs of ZnO with application of pressure during (a) complete dwell time and (b) start of dwell time until end of cooling cycle. (c) Start of dwell time and released at the end of dwell time with optimized temperature and time. Maximum pressure application during (d) start of heat cycle and held for complete experiment, (e) start of heat cycle and released during the cooling and (f) start of heat cycle and held only during heat cycle.

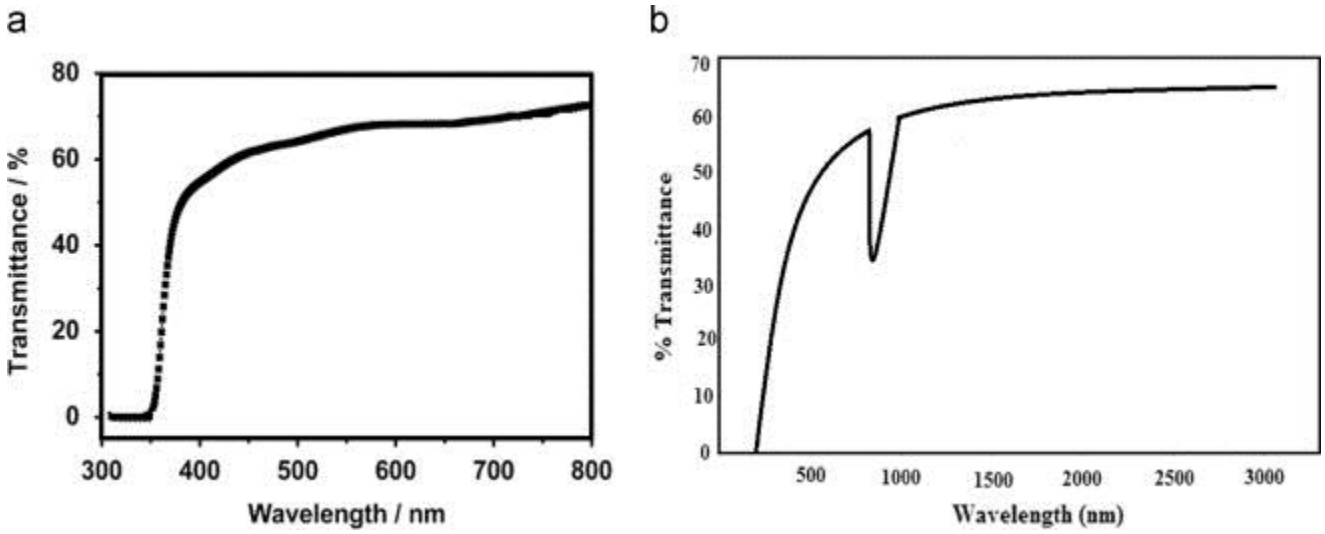

Fig. 5. Transmittance spectra of (a) ZnO ceramics sintered at 1100 °C for 20 min with heating rate of 10 °C/min and (b) YLO ceramics sintered at 1700 °C for 5 min with heating rate of 50 °C/min after annealing at 1200 °C.